100 year anniversary
Measurement Science and Technology

Finite element modelling for micro-scale thermal investigations using photo-thermal microscopy data inversion

View the article online for updates and enhancements.

You may also like

Finite element modelling for micro-scale thermal investigations using photo-thermal microscopy data inversion

L Autrique[1,2], L Perez[1] and J J Serra[2]

[1] Faculté des Sciences Exactes et Expérimentales, Université de Perpignan Via Domitia,
52 avenue Paul Alduy, 66860 Perpignan Cedex, France ,
[2] DGA/CEP/EHF, groupe Expertise Hauts Flux, BP 59, 66121 Font-Romeu Cedex, France

E-mail: autrique@univ-perp.fr, laetitia.perez@univ-perp.fr and serra.ghf@wanadoo.fr

Abstract
Within heterogeneous materials like fibre reinforced composites, heat
transfer is a complex phenomenon that depends on thermal properties of
both fibre and matrix materials and often thermal contact resistance between
them. In addition, the fibre axial and radial thermal behaviour is different
and both characteristics have to be investigated. In the present work, a
photo-thermal microanalysis method has been used to measure the fibre
thermal diffusivity when inserted inside a matrix. The experimental device
is based on a photo-thermal method in which periodic excitation is localized
on a micrometre-scale spot. Estimations of local properties are deduced
from the temperature evolution in a micrometre-scale zone and measured at
a given distance. In the case of fibre characterization, the composite sample
is cut along a plane perpendicular to the fibre axis for measuring the radial
diffusivity or containing the fibre axis for measuring the axial diffusivity.
With small diameter fibres, the thermally excited volume is larger than the
fibre itself and heat exchange with the matrix has to be taken into account.
In this case, the direct problem cannot be solved by an analytical approach; a
finite element method has been used. Numerical and experimental results
are compared.

Keywords: parametric identification, photo-thermal method, composite
materials, micro-scale characterization, phase lag analysis, finite element
method

(Some figures in this article are in colour only in the electronic version)

1. Introduction

The development of new methods capable of characterizing
the micro-scale thermal behaviour of heterogeneous complex
materials is a crucial step for elaboration optimization. In
such a way, an identification problem has to be investigated.
In [11], a direct problem is assumed that is a well-posed
problem of mathematical physics. In other words, if we
know completely a 'physical device', we have a classical
mathematical description of this device including uniqueness,
stability and existence of a solution of the corresponding
mathematical problem. But if one of the (functional)
parameters describing this device is to be found (from
additional boundary/experimental) data, then we arrive at
an inverse problem. Considering the previous definition,
parametric identification performed by inverse problem
resolution requires three main steps:

Step 1: formulation of a mathematical model describing
the direct problem. In most cases, numerical methods are
developed for system state prediction. Moreover, considering
sensitivity analysis derived from the direct problem, optimal

design is often achieved. Thus, reliable observations can be obtained.

Step 2: conception and validation of an experimental device in order to measure material behaviour when submitted to an excitation.

Step 3: minimization of the difference between predicted values (step 1) and measured values (step 2). In most cases, an iterative algorithm is implemented and unknown parameters are adjusted at every iteration.

The experimental device presented in this paper is based upon a periodic method dedicated to microscopic study. The sample is heated by a modulated laser beam on its surface and a temperature-dependent coefficient (optical reflectivity) is measured near the heating source. The distance to which heat has propagated during a period is called thermal diffusion length [19]. When modulation frequencies are higher than 10 kHz, the thermally excited volume does not exceed some μm^3. In this volume, the temperature wave is characterized by amplitude and phase lag—compared to the heating reference— of its periodic component. Since time-dependent solutions are numerically difficult to estimate (for high-frequency excitation), a complex temperature is considered which leads to the determination of both phase lag and modulus in the stationary state. The temperature evolution (induced by the periodic heating input) is the sum of a continuous component and a periodic one characterized by its amplitude and phase lag versus thermal excitation. With the optical reflectivity being temperature dependent, the phase lag between optical reflectivity variations and heating input depends on the thermal properties of the heated volume. Thus, it leads to the identification of the thermal diffusivity of the studied material in a microscopic area ($\leqslant 20\,\mu$m). This experimental device has been developed in order to study at a microscopic scale:

- thermal characteristics of materials (thermal property distribution, anisotropy, etc),
- thermal interfaces between multi-component materials,
- thermal discontinuities (cracks etc).

An inverse problem has to be solved in order to identify the thermal diffusivity of the studied material. Minimization of the difference between observed phase lag and simulated phase lag is performed. Simulated values are deduced from a mathematical model describing the heat transfer induced by periodic excitation. Semi-analytical solutions are proposed in [9, 18] for homogeneous samples and in [6, 15, 19] for several types of discontinuities. In [6], the partial differential equation system is solved considering the analogy between the Helmholtz equation and the Laplace transform of the heat diffusion equation in order to obtain the Laplace transform of the solution. Then, using the inverse Laplace transform the time evolution of the surface temperature heated by a short light pulse is found. In other specific configurations (axis symmetry etc), using a space Fourier transform, calculation of the inverse Fourier transform is carried out numerically and gives the temperature amplitude and phase lag values compared to the incident modulated heat flux. Bessel functions and Hankel transforms are also usual tools for semi-analytical solution determination. However, the validity of the semi-analytical solution sharply depends on a strong hypothesis which can be quite difficult

Table 1. Diffusion length estimation.

Frequency (Hz)	Diffusivity (m^2 s^{-1})	Diffusion length (μm)
$f = 10^4$	$a = 10^{-5}$	$\delta \approx 20$
$f = 10^6$	$a = 10^{-6}$	$\delta \approx 0.5$

to verify for heterogeneous materials. In fact, the distance which the heat has propagated during a period is called thermal diffusion length $\delta = \sqrt{a/\pi f}$, where a is the thermal diffusivity and f is the modulation frequency [19]. In the studied configuration, the thermally excited volume does not exceed some μm^3. When spatial heterogeneities dimension approaches the thermal diffusion length (see table 1), the semi-analytical solution is not valid.

For example, identification of thermal diffusivity in micrometric fibres, the diameter of which is less than $10\,\mu$m, is difficult to perform using an inverse Fourier transform. In such a framework, a numerical solution based on the finite element method (FEM) is proposed [2].

2. Modelling in the frequency domain

Thermal waves produced by periodic heat generation in homogeneous and inhomogeneous solids are examined from the theoretical point of view in [10]. Application to thermal diffusivity measurement is proposed, for example, in [6, 14, 17–19]. Let us consider the following notation: $\Omega_i \in \mathbb{R}^3$ is the space domain corresponding to the component i; $X = (x, y, z) \in \cup\Omega_i$ is the space variable; $t \in T$ is the time variable. In [15], the periodic heat flux focused on the surface Γ at point I is expressed in the form

$$\phi\,(r_X, t) = \phi_0\,\mathrm{e}^{-r_X^2/r_0^2}\,\mathrm{e}^{\mathrm{j}\omega t} \tag{1}$$

where ϕ_0 is the heat flux amplitude (W m^{-2}), r_X is the distance XI (in m), r_0 is characteristic of the heat flux spatial distribution (m), ω is the pulsation (rad s^{-1}). The evolution of temperature $\theta(X, t)$ in $\cup\Omega_i$ is described by the following equations,

$$\forall\,(X, t) \in \cup\Omega_i \times T \qquad \Delta\theta(X, t) - \frac{1}{\alpha_i}\,\frac{\partial\theta(X, t)}{\partial t} = 0 \tag{2}$$

where α_i is the unknown diffusivity,

$$\forall\,(X, t) \in \Gamma \times T$$
$$-\lambda_i\,\frac{\partial\theta(X, t)}{\partial\vec{n}} = \mathrm{Re}(\phi(r_X, t)) - h\theta(X, t) \tag{3}$$

where λ_i is the thermal conductivity, $\vec{n}$ is the normal vector exterior to Γ and h is the convective exchange coefficient,

$$\forall\,X \in \cup\Omega_i \qquad \theta(X, 0) = 0. \tag{4}$$

Since the heat flux is periodic on Γ, temperature variations in $\cup\Omega_i$ will be periodic as well. When the steady state is established, a continuous component and a periodic one are considered:

$$\theta(X, t) = \theta_c(X) + \theta_\omega(X)\,\mathrm{e}^{\mathrm{j}\omega t}. \tag{5}$$

In the following, the study is devoted to the periodic component, i.e. computation of its amplitude and phase lag

with respect to the incident flux. From (2)–(4), we obtain

$$\forall X \in \cup \Omega_i \qquad \Delta \theta_\omega(X) - \frac{j\omega}{\alpha_i}\theta_\omega(X) = 0 \qquad (6)$$

$$\forall X \in \Gamma \qquad -\lambda_i \frac{\partial \theta_\omega(X)}{\partial \vec{n}} = \phi(r_X) - h\theta_\omega(X) \qquad (7)$$

where

$$\phi(r_X) = \phi_0 \exp\left(-\frac{r_X^2}{r_0^2}\right).$$

In specific configurations such as homogeneous solid, semi-infinite geometries, temperature-independent parameters, particular multi-component configurations (for which thermal interfaces are well identified), calculation of the inverse Fourier transform (or Laplace inverse transform) leads to a semi-analytical solution; see theoretical aspects and applications in [5–7, 9, 14, 15, 17–19]. From the experimental point of view, for heterogeneous materials which do not verify previous assumptions, thermal diffusivity identification according to semi-analytical solution can lead to an erroneous estimation. In order to provide a general alternative for the resolution of equations (6), (7), the FEM is implemented.

A sensitivity study of an observable S on the model parameters $\beta = [\beta_1, \beta_2, \ldots, \beta_n]$ allows us either to reduce the forward model or to discuss the possibility of accurate identification of physical parameters [3]. Sensitivity functions are defined as the absolute variation of the observable induced by an absolute variation of the considered parameter. In order to compare these coefficients with each other, the reduced sensitivity functions of η versus parameter β are defined by the following relation: $X_{\beta_i}^* = \beta_i \frac{\partial S(\beta)}{\partial \beta_i}$. In the studied framework, a reduced sensitivity study of the modulus ($|\theta_\omega|$) and of the phase lag ($\varphi = \arg(\theta_\omega)$) on model parameters has been previously performed. This sensitivity study has been realized for the unknown parameters but also for the known parameters (which are *a priori* known with given uncertainties). These results are not presented but discussed all the same:

- Even if phase lag and modulus are calculated and/or measured, only the phase lag observations lead to a correct identification. In fact, the sensitivity study puts in evidence that the modulus is correlated not only with unknown thermal diffusivities but also with nuisance parameters (heat flux, convective heat losses, etc).
- Nevertheless, the convective heat losses h could be identified according to the modulus but their effects on phase lag observations $h\frac{\partial \varphi}{\partial h}$ are not significant enough to perturb the thermal diffusivity identification.
- It is important to accurately control the periodic excitation ω.

In the following, only phase lag predictions and measurements are exposed. Even if phase lag spatial distribution can be considered for thermal diffusivity identification [15], results are shown for frequency scanning. Phase lag is measured and computed at a given distance of the heating laser (on the material surface). Then from phase lag versus frequency, thermal diffusivity can be identified.

Table 2. Error estimation.

Metal (purity > 99.9%)	a_{lit} (mm² s⁻¹) (literature)	a_{meas} (mm² s⁻¹) (measured)	$|1 - a_{\text{lit}}/a_{\text{meas}}|$ (%)
Titanium	9.09	9	1
Rhenium	16.43	14	15
Platinum	25.46	29	14
Gold	125.75	112	11
Silver	172.98	191	10

3. Simulation and numerical result

3.1. Validation for homogeneous material

Let us consider a titanium sample. On its surface Γ_1, a Gaussian heating flux is considered: $\phi(r) = \phi_0 \exp\left(-\frac{r^2}{r_0^2}\right)$ where $\phi_0 = 5 \times 10^8$ W m⁻² and $r_0 = 1.5$ μm. Numerical results are shown considering the following thermo-physical parameters: $a = 9 \times 10^{-6}$ m² s⁻¹, $\lambda = 21.6$ W m⁻¹ K⁻¹ and $h = 10$ W m⁻² K⁻¹. Boundary conditions are (see figure 1)

$$\forall X \in \Gamma_1 \qquad -\lambda \frac{\partial \theta_\omega(X)}{\partial \vec{n}} = \phi(r_X) - h\theta_\omega(X)$$

$$\forall X \in \Gamma_2 \qquad -\lambda_i \frac{\partial \theta_\omega(X)}{\partial \vec{n}} = 0.$$

Figures are presented as follows:

- Figure 1: implemented meshes (initial mesh and refined mesh).
- Figure 2: phase lag versus excitation frequencies predicted by analytical approach [9] for several metallic materials.
- Figure 3: phase lag versus excitation frequencies and comparison between FEM approach and analytical approach [9] and measurements given by the experimental device presented in section 4.

For figure 2, thermal diffusivities of metallic materials are listed in table 2 from the values given in the literature. It is obvious that phase lag is strongly affected by thermal diffusivity. Thus, phase lag measurements can lead to thermal diffusivity identification and metallic sample recognition even if data are 'moderately' noise perturbed.

Considering figure 3, several remarks are proposed. Differences between the initial mesh (red curve) and the refined mesh (blue cross) are close to zero, so an unrefined mesh can be considered since numerical results are correct and computational time is smaller. Numerical predictions obtained from a semi-analytical approach are slightly different than those obtained from FEM. This could be due to the different numerical algorithms and to the heat flux $\phi(r)$ modelling which is Gaussian shape for FEM and cylindrical shape in [9]. Measurements performed with the photo-thermal microscope seem to be in good agreement with predicted results on the titanium sample.

3.2. Numerical results for heterogeneous material

Let us consider a cylindrical fibre (radius r_f) inside a matrix. In most cases, fibre diffusivity and matrix thermal diffusivity
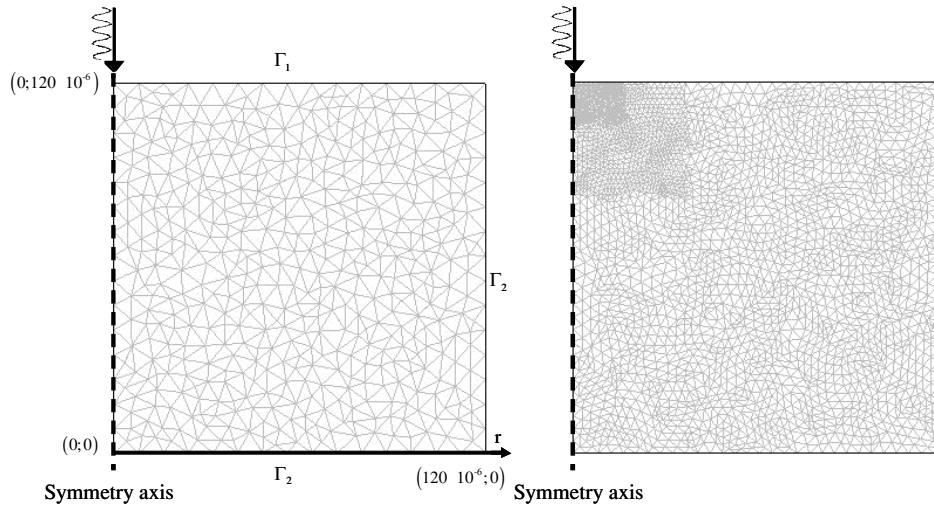
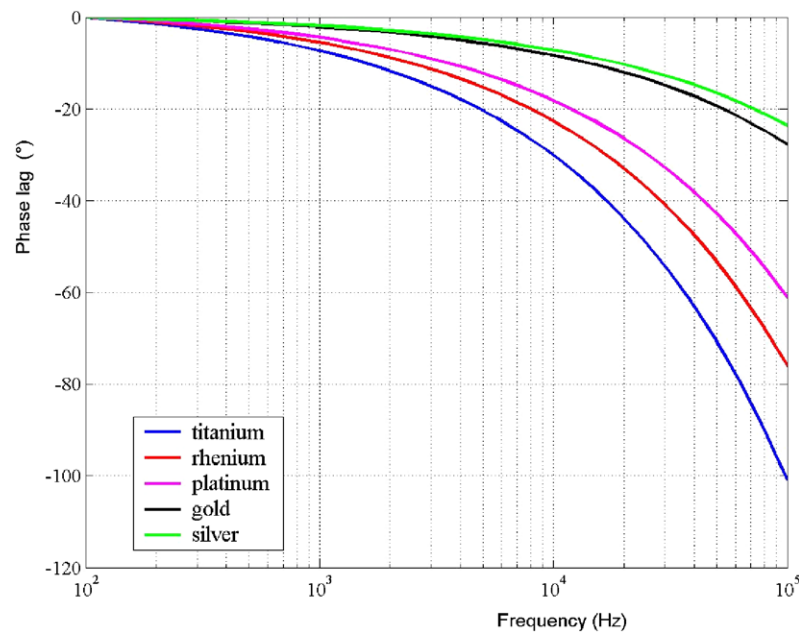**Figure 1.** Initial and refined mesh for the titanium sample.

Figure 2. Phase lag versus frequency for several metallic materials.

are quite different. When diffusion length is smaller than the fibre radius ($\delta \ll r_f$), the boundary effect due to the matrix can be neglected and a semi-analytical approach can be implemented. However for a small fibre radius, a semi-analytical approach can lead to erroneous estimates since thermal waves propagation is different in fibre and matrix.

The investigated geometry is shown in figure 4. In figures 5 and 6, results are shown for $4 \, \mu\text{m} \leqslant r_f \leqslant 35 \, \mu\text{m}$, observations are performed on the surface Γ_1 (distance to the axis equal to $3 \, \mu\text{m}$) and the excitation frequency is equal to 1 kHz, 10 kHz and 100 kHz. The following parameters are taken into account: in figure 5 $a_{\text{fibre}} = 10^{-6} \, \text{m}^2 \, \text{s}^{-1}$ and $a_{\text{matrix}} = 20 \times 10^{-6} \, \text{m}^2 \, \text{s}^{-1}$, and in figure 6 $a_{\text{fibre}} = 20 \times 10^{-6} \, \text{m}^2 \, \text{s}^{-1}$ and $a_{\text{matrix}} = 10^{-6} \, \text{m}^2 \, \text{s}^{-1}$.

Remarks

- Figure 5: for the studied case where $a_{\text{fibre}} < a_{\text{matrix}}$, at a high frequency (100 kHz) diffusion length is $\delta \approx 1.8 \, \mu\text{m}$ and for $r_f > 3\delta \approx 5.4 \, \mu\text{m}$ phase lag in the fibre is not affected by the matrix properties. For $r_f < 3\delta$, boundary effects cannot be neglected and the maximal difference is about $4°$. For a medium frequency (10 kHz), $\delta \approx 5.6 \, \mu\text{m}$, the same fibre radius threshold (equal to 3δ) can be taken into account in order to neglect boundary effects. For a low frequency (1 kHz), smaller phase lags are obtained and one can see that for a small fibre radius, matrix properties cannot be neglected.

- Figure 6: for the studied case where $a_{\text{fibre}} > a_{\text{matrix}}$, at a high frequency (100 kHz) diffusion length is $\delta \approx 8 \, \mu\text{m}$
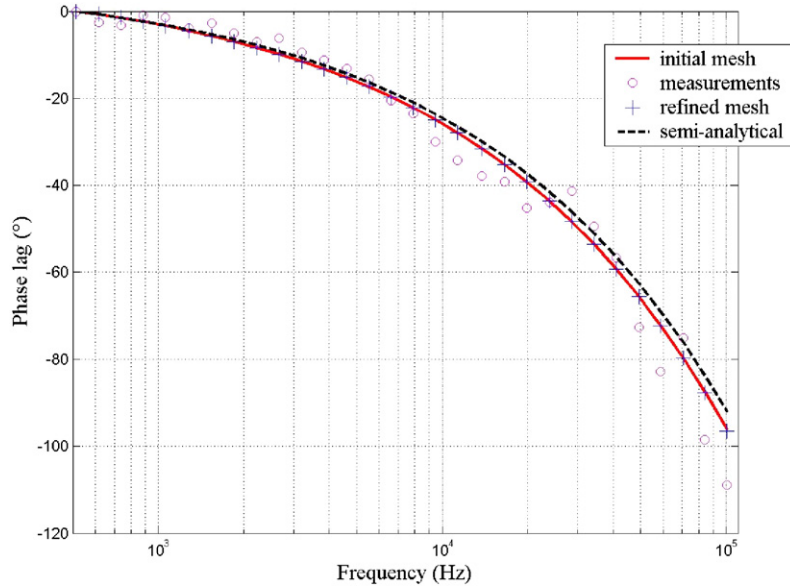
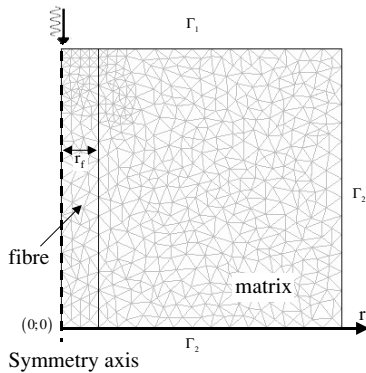**Figure 3.** Phase lag versus frequency for the titanium sample (observations for $r = 10\,\mu$m).

Figure 4. An example of a heterogeneous material.

and for $r_f > 3\delta \approx 24\ \mu$m phase lag in the fibre is not affected by the matrix properties. For $r_f < 3\delta$, boundaries effects cannot be neglected and the maximal difference is about $5°$. For a medium frequency (10 kHz), $\delta \approx 25\ \mu$m, and a low frequency (1 kHz), $\delta \approx 79\ \mu$m, matrix properties cannot be neglected for a small fibre radius.

Thus, considering the results shown in figures 5 and 6, a semi-analytical approach (assuming in [9] that the material is homogeneous) can lead to erroneous estimates of the thermal diffusivity for a small fibre radius. For the investigated examples, FEM has to be implemented for $r_f < 3\delta = 3\sqrt{a_{\text{fibre}}/(\pi f)}$.

In the following, the effect of the difference between matrix and fibre thermal diffusivities is studied. Let us consider $a_{\text{fibre}} = 10^{-5}$ m^2 s^{-1} and ratio $0.1 \leqslant \frac{a_{\text{fibre}}}{a_{\text{matrix}}} \leqslant 10$. The fibre radius is $r_f = 10\ \mu$m, observations are performed on the surface Γ_1 (distance to the axis equal to $3\ \mu$m), and the excitation frequency is equal to 1 kHz, 10 kHz and 100 kHz. Results are presented in figure 7.

In this situation, numerical results provided by the semi-analytical approach are correct for $\frac{a_{\text{fibre}}}{a_{\text{matrix}}} = 1$ since the

materials are identical (from the phase lag point of view). However, for fibre thermal diffusivity, quite different from matrix thermal diffusivity, phase lags estimated by FEM differ from homogeneous material. Moreover, at low frequency and high frequency, phase lag difference behaviour is not the same. Thus while drawing phase lag versus frequency (as in figure 2) the curve shape is different when a_{fibre} and a_{matrix} are significantly different.

Numerical results presented in section 3.1 (for homogeneous materials) and section 3.2 (for heterogeneous materials), validate the predictions obtained by FEM and show that an unrefined mesh can lead to good estimations. Moreover, limitations of the semi-analytical approach [9] are exposed for a small fibre radius and when fibre thermal diffusivity and matrix thermal diffusivity differ. Thus for identification purposes, FEM is implemented in specific configurations investigated by photo-thermal microscopy. The experimental device is exposed in the following section.

4. Experimental device

The experimental device used for obtaining measurements able to characterize the micro-scale thermal behaviour of heterogeneous materials is a versatile photo-thermal microscope. Although the principle of such a device is well known since Rosencwaig *et al* [16], it will be recalled in order to point out its main advantages and drawbacks.

4.1. Description

The measurement technique is based on the sample's thermal response when it is submitted to a micro-scale periodic thermal excitation. A modulated laser beam (pump), focused by a microscope objective onto the sample surface, produces a local thermal excitation ($\approx 1\ \mu$m diameter spot). At a given distance (≈ 4–$5\ \mu$m), a continuous laser beam (probe) is used
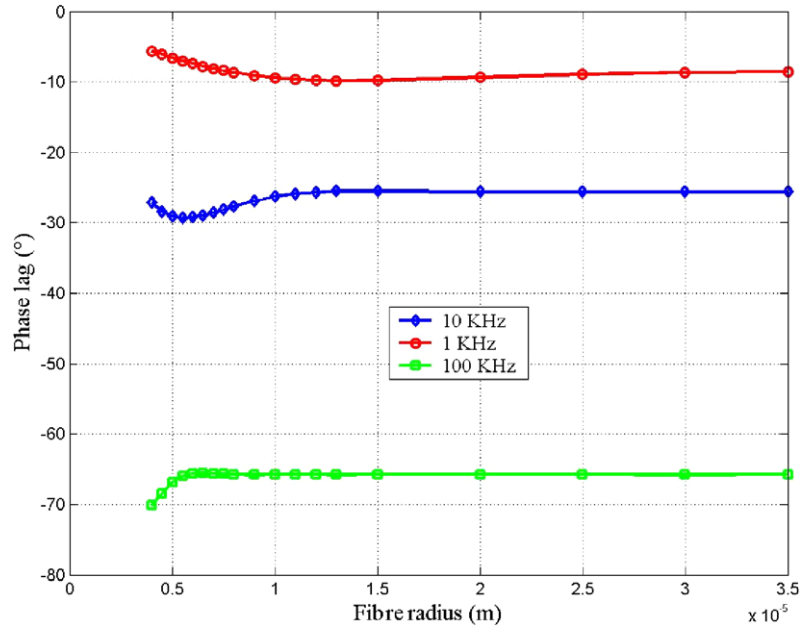
Figure 5. Phase lag for $a_{\text{fibre}} = 10^{-6}$ m^2 s^{-1} and $a_{\text{matrix}} = 20 \times 10^{-6}$ m^2 s^{-1}.
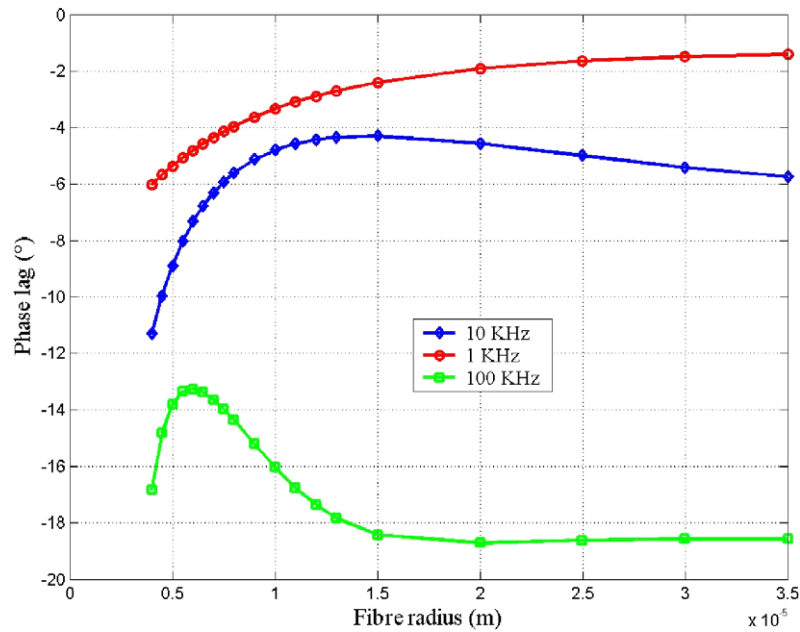
Figure 6. Phase lag for $a_{\text{fibre}} = 20 \times 10^{-6}$ m^2 s^{-1} and $a_{\text{matrix}} = 10^{-6}$ m^2 s^{-1}.

to detect the thermal wave diffusion by observing the variations of the surface optical reflectivity that depend on temperature [4, 7, 13]. In our experiment (see figures 8 and 9), the thermal excitation is delivered by an ion-argon laser (Coherent, Innova 305) with its 514 nm wavelength selected.

An acousto-optic modulator (Isomet 1211) driven by a computer-programmable function generator and a RF amplifier modulates the beam at the desired frequency. After shape setting, the beam is reflected by a dichroic plate and focused by a microscope objective (50×, Mitutuyo) on a Gaussian micro-scale spot at the sample surface. The 632 nm measurement beam, originated from a He–Ne laser

(Oriel 79200), crosses a polarization beam-splitter and the dichroic plate, then is directed to the same objective which focuses it close to the heating spot. The distance between spots (called offset) is accurately adjusted by means of wedge prism rotation. The reflected part is sent back to the polarization beam-splitter which reflects it towards a fast response photodiode. The photodiode ac component signal is amplified and analysed by a wide bandwidth lock-in device (EGG 5302), the reference signal of which comes from the acousto-optic controller. The lock-in amplifier output (amplitude and phase lag) is finally recorded by the control computer. The phase lag between optical reflectivity
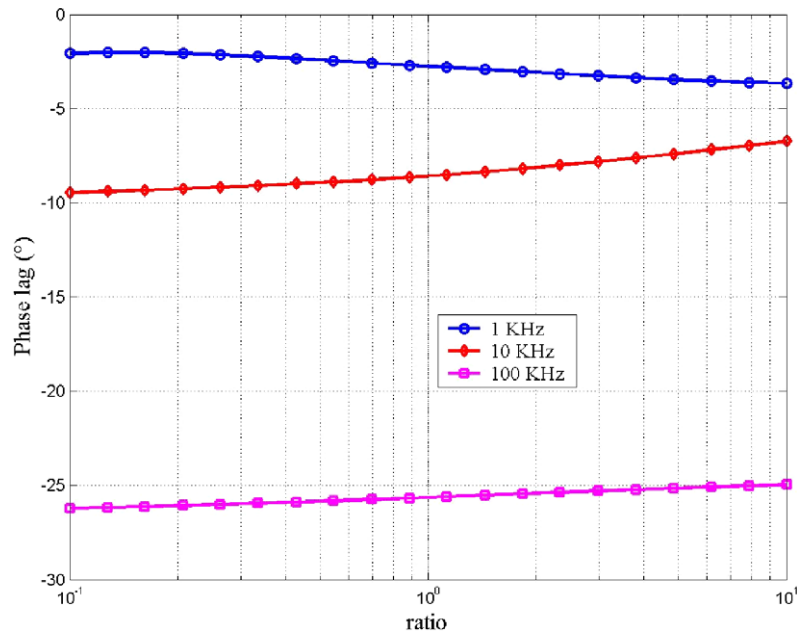
Figure 7. Phase lag for $0.1 \leqslant \frac{a_{\text{fibre}}}{a_{\text{matrix}}} \leqslant 10$.
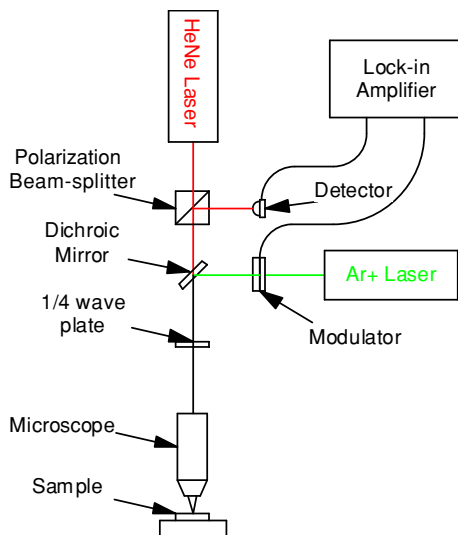

Figure 8. Schematic drawing of the photo-thermal microscope.

variations and heating laser modulation corresponds to the thermal diffusion process between excitation (pump) and observation (probe) spots.

The unknown thermo-physical properties are thus micro-scale characteristics of the investigated zone. These properties are then identified by analysing the evolution of the phase lag versus an adjustable parameter (independent variable) such as excitation frequency, distance between spots or distance from a thermal discontinuity.

4.2. Calibration procedure

The experimental system (optical and electronic devices) introduces an additional phase shift that should be subtracted from the measured value to keep only the thermal contribution. For that purpose, a calibration procedure consists in picking up

with an optical fibre a small part of the pump beam and sending it directly to the detector. The resulting phase, measured on the whole frequency range, is stored in a table that will be used to correct the set of experimental values obtained from the samples. Because of the short distance between pump and probe spots, their shape and size are to be taken into account. Although commercially available beam analysers do allow measurements of micro-scale beams, they are not adapted for analysing beams focused by such high numerical aperture objectives. The spot characteristics are investigated by a two-step procedure [5]. A scanning slit beam profiler (Data Ray Beamscope P5) capable of measuring focused beam profiles of some tens of micrometres is used to analyse the beam shape in several locations upstream and downstream of the waist. This step allows the verification of the beams' Gaussian shape and the determination of their quality coefficient. It then becomes possible to extrapolate the value of the waist diameter by applying the Gaussian beam propagation law. Analysis performed on the system equipped with the specified objective (50×, Mitutuyo) gives the following results:

- Pump spot diameter: $1.00 \pm 0.04 \ \mu$m.
- Probe spot diameter: $1.24 \pm 0.04 \ \mu$m.

4.3. Sample holder and positioning

The sample is held by a two-stage micro-positioning system (0.1 μm resolution) driven by the computer. This allows one-dimensional (1D) scanning of the sample surface that will be used for thermal parameter estimation, or two-dimensional (2D) scanning for imaging the map of surface thermal transfers. Heterogeneous samples often comprise materials of different hardness and so the polishing results in surface altitude variations of some micrometres. Because of the low depth-of-field, these variations have to be corrected. The sample holder involves a third movement in the r-direction so as to maximize the probe laser reflected beam.
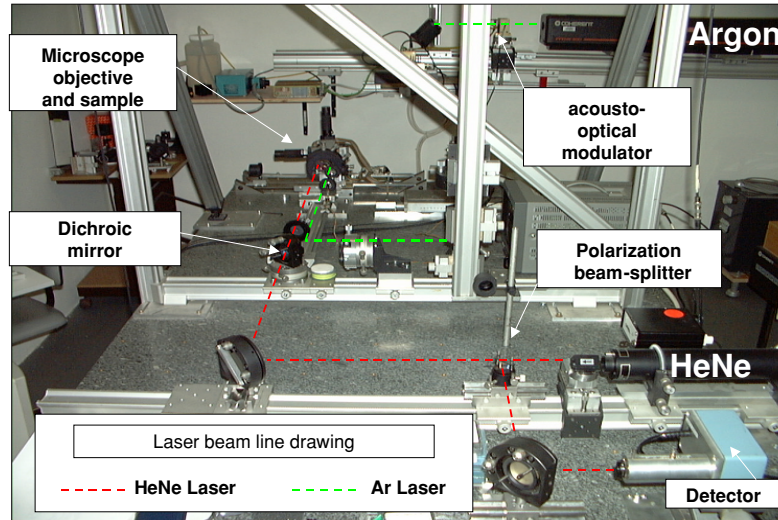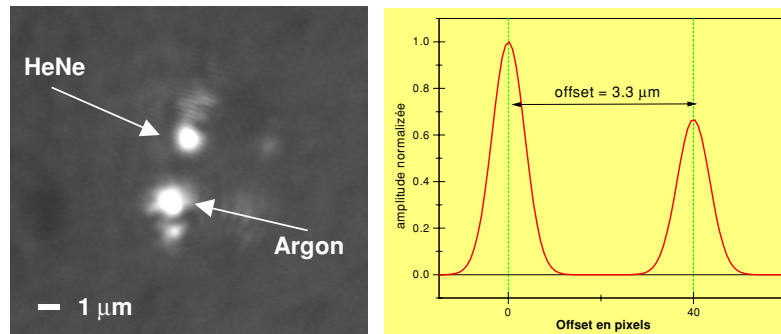
Figure 9. Photo-thermal microscope.

Figure 10. An example of a surface image.

A CCD camera sights the surface by means of a beam-splitter. Its aim is an accurate positioning of both spots on the sample surface as well as a measurement of distance between the spots. (Note that the disturbing reflections observed in figure 10 come from colour filters and not from the surface.) The various illumination levels (pump and probe spots, surface lighting) are very different and so a raw image would be saturated and unusable. In order to balance them, the surface is lightened by a pulsed 932 nm diode and the composite beam reflected by the surface passes through colour filters attenuating the 514 nm and 632 nm wavelengths.

5. Identification algorithm

Once the thermal model is established (section 2) and the direct problem is numerically solved (section 3), measurements obtained by the experimental device (section 4) are taken into account for parametric identification. It is essential to note that as well as the hypothesis required for semi-analytical solutions validity not being verified, the well-known linear relation between phase lag and excitation frequency is not valid either. Then, an identification procedure has to be developed in order to estimate thermal diffusivity by minimizing the difference between simulated phase lag (figure 5) and measured phase lag (figure 11). For the resolution inverse problem, one can refer to [1, 3, 11, 20].

5.1. Numerical results

In this section, measured phase lags are considered in order to identify both fibre and matrix thermal diffusivity. Let us consider noisy simulated data for identification algorithm validation. The first step is to identify matrix thermal diffusivity ($a_{\text{matrix}} = 10^{-7}\ \text{m}^2\ \text{s}^{-1}$). The Levenberg–Marquardt algorithm is implemented (Matlab® and Femlab®) in order to minimize in a least-squares sense the quadratic difference between the measured and simulated phase lags. Results are shown in figure 10. Once a_{matrix} is identified, measurements are performed in order to identify the thermal diffusivity ($a_{\text{fibre}} = 10^{-5}\ \text{m}^2\ \text{s}^{-1}$) of the fibre (radius 4 μm). Results are shown in figure 11.

Remarks. The Levenberg–Marquardt algorithm implemented for the matrix's thermal diffusivity identification provides efficient minimization. In figure 12, it is crucial to consider simulated phase lags obtained by the FEM approach. In fact, the dashed line corresponds to $a_{\text{fibre}} = 10^{-5}\ \text{m}^2\ \text{s}^{-1}$ in a semi-infinite domain which verifies the geometrical assumptions required by the semi-analytical approach. In the studied
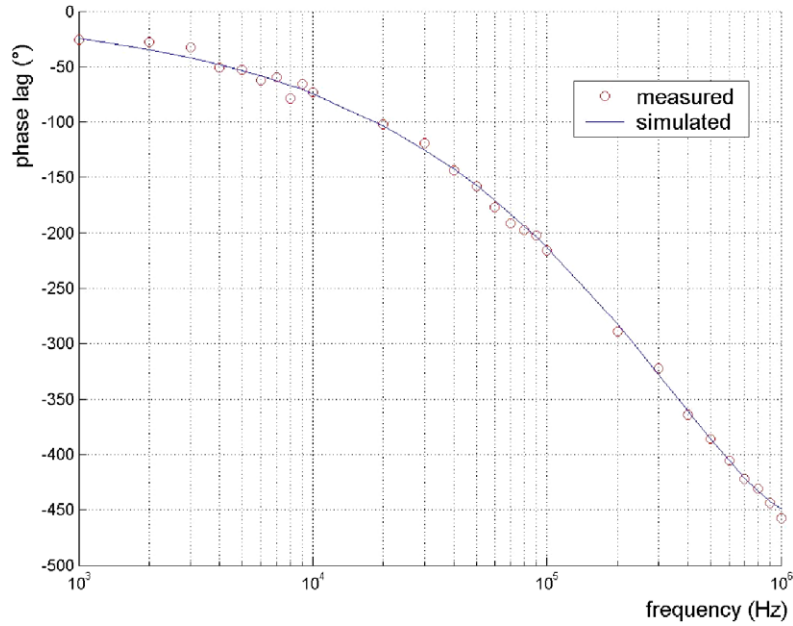
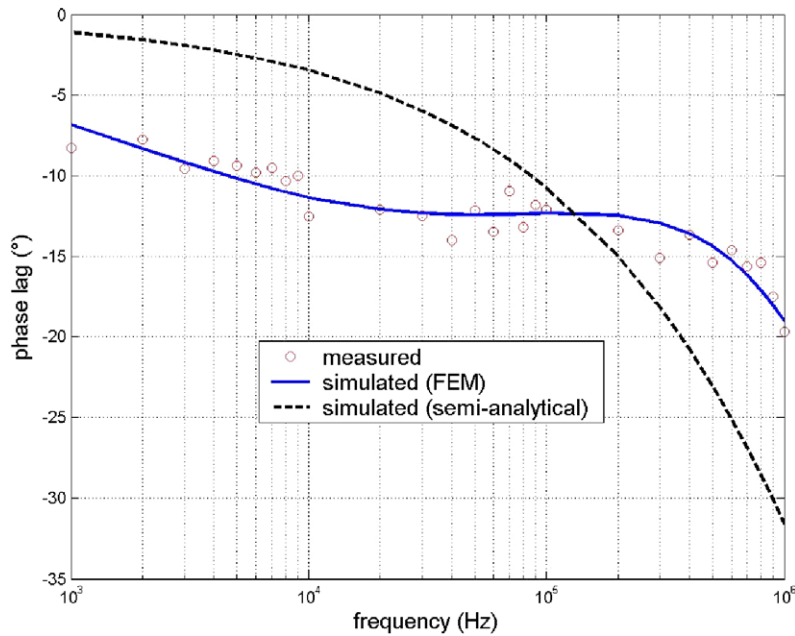**Figure 11.** Matrix thermal identification from noisy simulated data (observations for $r = 6.17\,\mu$m).

Figure 12. Fibre thermal identification from noisy simulated data (observations for $r = 3\,\mu$m).

situation, the small fibre radius (4 μm) prevents us neglecting the matrix environment. Thus, minimization based on the semi-analytical approach and linear relation between phase lag and excitation frequency will lead to erroneous estimation of the fibre's thermal diffusivity.

5.2. Estimation errors

If β and $\hat{\beta}$ are respectively the exact value and the estimated value of the parameter vector, the estimation error e_β stems generally from several sources:

- *Errors due to numerical modelling (round, truncation).* When the direct model has an analytic solution, this type

of error can be neglected because, by definition, the exact analytic solutions are exact and the round errors on the phase are much lower than the resolution of the lock-in amplifier, i.e. $0.01°$. When the direct model has a semi-analytic solution (includes an integral to be calculated numerically), the truncation error is not so difficult to evaluate. In the case of use of a finite element method, the choice of mesh, space steps, etc are to be taken into account.

- *Errors on model assumptions.* The model is based on a series of assumptions: flat sample, Gauss distribution of the heat source, negligible heat losses (in this frequency range), constant thermal parameters (in this
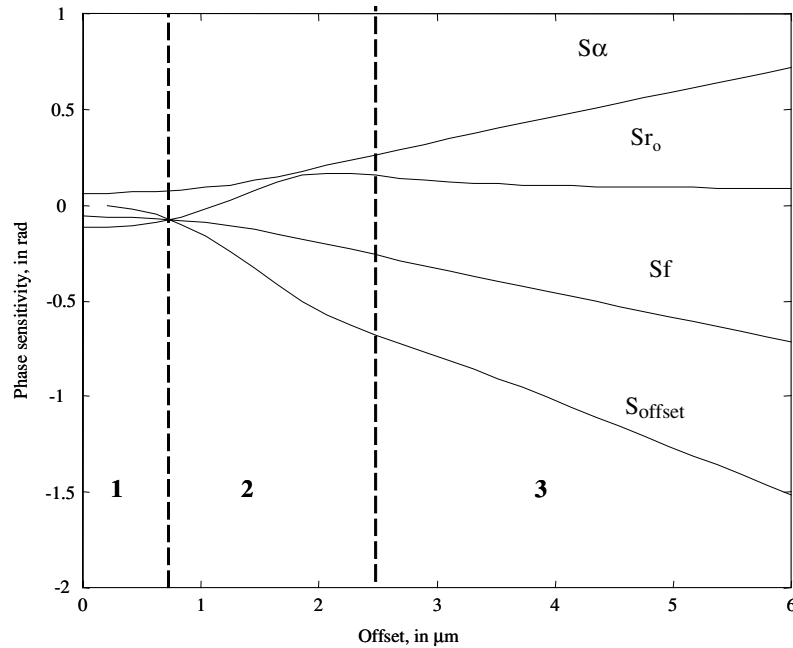
9

Figure 13. Errors of supposed known parameters.

temperature range), steady stage regime, etc. Each of these assumptions has been analysed and validated for actual cases. In addition, the estimation residuals are systematically investigated in order to seek a possible 'signature' that would be the sign of a wrong assumption [3].

- *Errors due to measurement noise.* A useful tool for estimating the effect of the measurement noise on the estimated uncertainty is the Cramer–Rao inequality. Under some assumptions concerning the noise nature, this theorem (1) express a lower bound for the variance of any unbiased estimator of β and (2) gives the existence condition of an estimator reaching this bound. In this case, the estimator is qualified as MVU (minimum variance unbiased) [12]. A detailed analysis of the measurement noise and application of the two cases (constant variance or linearly dependent variance with frequency) with different estimators (least-squares, Gauss–Markov, etc) is given in [8].

- *Error related to metrology.* With the observable parameter being the thermal phase lag, precautions have to be taken in order to avoid additional phase lags introduced by the measurement chain: function generator, acousto-optic modulator, photodiode, differential amplifier. The sum of these potential phase lags is measured by sending the attenuated heating beam directly to the measurement photodiode. Then, the table obtained for a series of frequency values is used to correct all the experimental photo-reflection data. Note that the resolution of the measurement device (lock-in amplifier) is $0.01°$, so more than enough compared to the other error sources.

- *Errors in supposed known parameters.* This component is investigated by analysing the reduced sensitivities of the supposed known parameters and parameters to be estimated [3]. Figure 13 shows, for a Gaussian source of radius r_0, the evolution of the different sensitivity coefficients: diffusivity, frequency, offset (the distance between the two lasers) versus the offset distance r. Three zones can be distinguished in these curves:

- For small r values, the sensitivity is low for all parameters.
- The sensitivity to spot radius passes a maximum for a value close to that of the diameter.
- For large r values, the results tend to that of the spherical model. The sensitivities to parameters a, r and f are correlated such that $S_a = -S_f = -0.5S_r$. The identifiable group is $\frac{r}{\delta}$.

An accurate knowledge of the offset is the most critical parameter.

The sum of these potential errors has been evaluated for an example of experiment: $\alpha = 10$ mm^2 s^{-1}, $r = 5$ μm, $r_0 = 0.62$ μm. The upper bound for e_β is 30%. In fact, measurements on standard samples show that the error is always lower than 15%.

6. Concluding remarks

In this paper, the interest of a finite element approach in parametric identification is presented. An experimental device (dedicated to microscopic-scale study) is developed for the identification of thermal diffusivity in heterogeneous materials. To estimate this property, a direct model is presented and resolution by the FEM is proposed in order to improve the identification when semi-analytical solutions cannot be considered. Thus, this experimental device (dedicated to micro-scale thermal diffusivity characterization) associated with our numerical approach (dedicated to complex temperature estimation) allows us to investigate heterogeneous

materials. In further works, this methodology has to be performed for thin interface characterization (in specific coated materials, for example) as well as for thermal discontinuities detection (for example, in crack formation due to thermal and mechanical cycling).

References

[1] Alifanov O M 1994 *Inverse Heat Transfer Problems* (Berlin: Springer) p 348

[2] Autrique L and Serra J J 2003 On the implementation of a finite element method for parameter identification *LUXFEM 2003: Int. Conf. on Finite Elements Applications* (*Luxembourg*) (CD-ROM)

[3] Beck J V and Arnold K J 1977 *Parameter Estimation in Engineering and Science* (New York: Wiley)

[4] Dilhaire S, Grauby S, Claey W and Batsale J C 2004 Thermal parameters identification of micrometric layers of microelectronic devices by thermoreflectance microscopy *Microelectron. J.* **35** 811–6

[5] Gagliano O, Commandré M, Suzanne P and Serra J J 2001 Maîtrise des paramètres optiques pour l'identification des propriétés thermiques à micro-échelle *Proc. OPTIX 2001* (*Marseille, France, 26–28 Nov.*)

[6] Garrido F, Salazar A, Alonso F and Saez-Ocariz I 2005 Characterization of buried cylinders and spheres by pulsed infrared thermography *J. Appl. Phys.* **98** 103502

[7] Gervaise C, Gagliano O, Serra J J, Claudet B, Commandré M and Serror S 2001 Local thermal characterization of inner gun barrel refractory metallic coatings *Microscale Thermophys. Eng. J.* **5** 209–23

[8] Gervaise C, Nouals C, Calderan C, Bénet S and Serra J J 1999 Thermal properties estimation by periodic heating methods: multi-scale approach *METTI Winter School* (*Odeillo, Jan.*) (in French)

[9] Gervaise C, Nouals C, Serra J J, Calderan C and Claudet B 1997 Diffusivity measurements by periodic methods *Proc. 24th Int. Thermal Conductivity Conf.* (*Pittsburgh, PA, USA, Oct.*) pp 229–40

[10] Gurevich Y G, Logvinov G N, de la Cruz G G and Lopez G E 2003 Physics of thermal waves in homogeneous and inhomogeneous (two-layer) samples *Int. J. Therm. Sci.* **42** 63–9

[11] Isakov V 1998 *Inverse Problems for Partial Differential Equations* (Berlin: Springer)

[12] Kay S M 1993 *Fundamentals of Statistical Signal Processing—Estimation Theory* (Englewood Cliffs, NJ: Prentice-Hall)

[13] Milcent E, Benet S, Gervaise C, Nouals C and Serra J J 1998 Microdiffusivity measurement on refractory metal coatings by photothermal microscopy *High Temp.—High Pressures* **30** 85–90

[14] Muscio A, Bison P G, Marinetti S and Grinzato E 2004 Thermal diffusivity measurement in slabs using harmonic and one-dimensional propagation of thermal waves *Int. J. Therm. Sci.* **43** 453–63

[15] Pruja P, Bénet S, Claudet B, Faugeroux O and Serra J J 2004 Photothermal microanalysis of thermal discontinuities in metallic samples *Superlatt. Microstruct.* **35** 409–18

[16] Rosencwaig A, Opsal J, Smith W L and Willenborg D L 1986 Detection of thermal waves through modulated optical transmittance and modulated optical scattering *J. Appl. Phys.* **59** 1392–4

[17] Salazar A and Sanchez-Lavega A 1994 Thermal diffusivity measurements using linear relations from photothermal wave experiments *Rev. Sci. Instrum.* **5** 2896–900

[18] Salazar A, Sanchez-Lavega A, Ocariz A, Guitonny J, Pandey C, Fournier D and Boccara A C 1996 Thermal diffusivity of anisotropic materials by photothermal methods *J. Appl. Phys.* **79** 3984–93

[19] Salazar A, Sanchez-Lavega A and Terron J M 1998 Effective thermal diffusivity of layered materials measured by modulated photothermal techniques *J. Appl. Phys.* **84** 3031–41

[20] Walter E and Pronzato L 1997 *Identification of Parametric Models from Experimental Data* (Berlin: Springer)